

Radiative Neutrino Mass Model at the e^-e^+ Linear Collider

Amine Ahriche,^{1,2,*} Salah Nasri,^{3,4,†} and Rachik Soualah^{5,‡}

¹*Department of Physics, University of Jijel, PB 98 Ouled Aissa, DZ-18000 Jijel, Algeria.*

²*International Centre for Theoretical Physics, Strada Costiera 11, I-34014, Trieste, Italy.*

³*Physics Department, UAE University, POB 17551, Al Ain, United Arab Emirates.*

⁴*Laboratoire de Physique Theorique, ES-SENIA University, DZ-31000 Oran, Algeria.*

⁵*INFN Sezione di Trieste, Gruppo Collegato di Udine,
University of Udine, via delle Scienze, 208, I-33100 Udine, Italy.*

We study the phenomenology of a Standard Model (SM) extension with two charged singlet scalars and three right handed (RH) neutrinos at an electron-positron collider. In this model, the neutrino mass is generated radiatively at three-loop, the lightest RH neutrino is a good dark matter candidate; and the electroweak phase transition strongly first order as required for baryogenesis. We focus on the process $e^+ + e^- \rightarrow e^- \mu^+ + E_{miss}$, where the model contains new lepton flavor violating interactions that contribute to the missing energy. We investigate the feasibility of detecting this process at future e^-e^+ linear colliders at different center of mass energies: $E_{CM} = 250, 350, 500$ GeV and 1 TeV.

I. INTRODUCTION

The Standard Model (SM) of elementary particle physics is very successful in explaining physics around the electroweak scale. However, Despite several questions remain to be answered such as neutrino masses and mixing [1], the nature of the dark matter (DM) [2] and the origin of the baryon asymmetry of the universe [3]. None of these issues is successfully explained within the SM. Therefore, various extensions beyond the SM have been proposed to address these problems.

In Ref. [4], Krauss, Trodden and one of the authors in this paper, proposed an extension of the SM with two charged $SU(2)_L$ singlet scalars and one right handed (RH) neutrino field, N_1 , where a \mathbb{Z}_2 symmetry was imposed at the Lagrangian level in order to forbid the Dirac neutrino mass terms. After the breaking of the electroweak symmetry, neutrino masses are generated at three-loop, which makes their masses naturally small due to the high loop suppression. Moreover, the field N_1 is odd under \mathbb{Z}_2 symmetry, and thus it is guaranteed to be stable, which makes it a good candidate for DM. Ref. [5] studied the phenomenological implication of this model with two RH neutrinos, instead of just one. In [6], it was shown that in order to fit the neutrino oscillation data and be consistent with different recent experimental constraints such as lepton flavor violation (LFV), one needs to have three RH neutrinos. A somewhat similar class of three-loop neutrino mass models has also been studied in [7].

In this work, we consider the feasibility of testing this radiative model at the next-generation electron-positron linear colliders [8–12]. The ILC, being designed for operation at several e^-e^+ collision energies, will be a great opportunity to anticipate detailed physics studies of our model. Among the different processes which can be studied at the ILC, we will focus here on the process $e^-e^+ \rightarrow e^- \mu^+ + E_{miss}$ within the allowed kinematic regions of the machine. Accordingly, our signal will consist of electron, anti-muon and missing energy. In the SM, the missing energy is coming just from one source $E_{miss}^{(SM)} \equiv \bar{\nu}_e \nu_\mu$, whereas in our model, there are twelve different processes that give rise to E_{miss} in the final state: six with SM left handed (LH) neutrinos and six contributions with heavy RH Majorana neutrinos. Moreover, the background process in our model gets modified through extra additional channels. Thus, we look for the excess in the number of events from the process $e^-e^+ \rightarrow e^- \mu^+ + E_{miss}$ in this model over the contribution from the SM and then identify whether the missing energy is produced from LH or RH neutrinos. Similar effects have been investigated in other class of models [13, 14].

This paper is organized as follows: in section II, we introduce the three-loop radiative model for neutrino masses, then we discuss its detectability at linear collider in section III. In section IV, we present and discuss the simulation results. We give our conclusion in section V.

*Electronic address: aahriche@ictp.it

†Electronic address: snasri@uaeu.ac.ae

‡Electronic address: rsoualah@cern.ch

II. THE MODEL

The model that we will study is an extension of the SM with three RH neutrinos, N_i , and two electrically charged scalars, S_1 and S_2 , that are singlet under $SU(2)_L$ gauge group in addition to a discrete \mathbb{Z}_2 symmetry, under which $\{S_2, N_i\} \rightarrow \{-S_2, -N_i\}$, and all other fields are even. The Lagrangian reads [6]

$$\mathcal{L} = \mathcal{L}_{SM} + \{f_{\alpha\beta} L_\alpha^T C i\tau_2 L_\beta S_1^+ + g_{i\alpha} N_i^C \ell_{\alpha R} S_2^+ + \frac{1}{2} m_{N_i} N_i^C N_i + h.c\} - V(\Phi, S_1, S_2), \quad (1)$$

where L_α is the LH lepton doublet, $f_{\alpha\beta}$ are the Yukawa couplings which are antisymmetric in the generation indices α and β , m_{N_i} are the Majorana RH neutrino masses, C denotes the charge conjugation operator, and $V(\Phi, S_1, S_2)$ is the tree-level scalar potential which is given by

$$V(\Phi, S_{1,2}) = \lambda \left(|\Phi|^2 \right)^2 - \mu^2 |\Phi|^2 + m_1^2 S_1^* S_1 + m_2^2 S_2^* S_2 + \lambda_1 S_1^* S_1 |\Phi|^2 + \lambda_2 S_2^* S_2 |\Phi|^2 + \frac{\eta_1}{2} (S_1^* S_1)^2 + \frac{\eta_2}{2} (S_2^* S_2)^2 + \eta_{12} S_1^* S_1 S_2^* S_2 + \{\lambda_s S_1 S_1 S_2^* S_2^* + h.c\}, \quad (2)$$

with Φ denotes the SM Higgs doublet. It has been shown that this model has the following features [6]:

- Small non-zero neutrino masses are generated radiatively at three-loop as shown in Fig. 1, which fits the neutrino oscillation data and without being in conflict with sever experiential constraints such as the bounds on lepton flavor violating processes, the muon anomalous magnetic moment and the neutrino-less double beta decay.
- Has a DM candidate (N_1) with a relic density in agreement with the observation for masses around the electroweak scale.
- Gives rise to strong first order phase transition that is required for a successful baryogenesis without being in conflict with the recent Higgs mass measurements provided by the ATLAS [15] and CMS [16] collaborations.
- Possible enhancement in the Higgs decay channel $h \rightarrow \gamma\gamma$, while the channel $h \rightarrow \gamma Z$ gets a small suppression within 5% according to the SM.
- Significant large enhancement on the triple Higgs coupling due to the extra contributions.

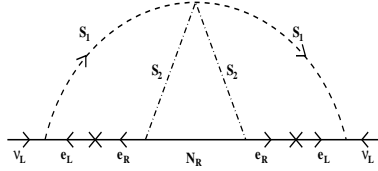


FIG. 1: The three-loop diagram that generates the neutrino mass matrix elements.

III. PHENOMENOLOGY AT LINEAR COLLIDERS

Neutrinos, which manifest inside the detector as missing energy, are produced due to the new lepton flavor violating interactions given by the f and g terms in (1). At an e^-e^+ linear collider such as the ILC, they can be directly pair-produced in association with a single (or multiple) photon(s), or a pair of charged leptons¹. In addition, both light (ν_i) and heavy (N_i) neutrinos can be generally produced at linear colliders according to their production cross section. However, by using polarized beams, one can reduce/increase the production rate of one type of chiral particles as compared to the other ones. For instance, if one uses LH polarized electron beam, the heavy RH Majorana neutrinos production rate gets suppressed and vice-versa. First, we will concentrate on the process $e^-e^+ \rightarrow e^-\mu^+ + E_{miss}$ considering unpolarized beams for different center of mass (CM) energies, E_{CM} , that can be accessible at the ILC. Second, we generalize our analysis by allowing for the possibility of tuning the beam polarization at the linear colliders.

¹ At the LHC, the LH (RH) neutrino can be produced via the decay of the charged scalar S_1 (S_2). However, the production rate of $S_{1,2}$ is expected to be small at the LHC.

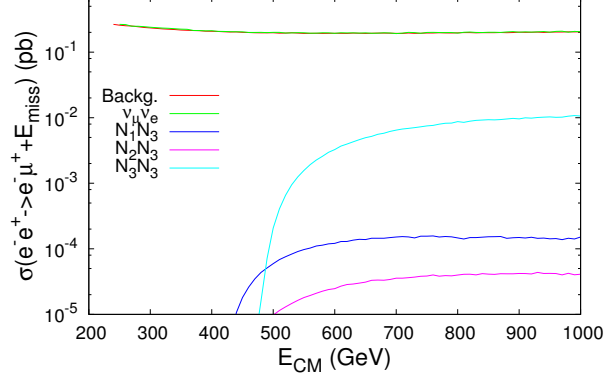


FIG. 2: The cross section of different contributions $\sigma(\mathcal{E}_{miss})$ versus the center of mass energy. The difference between the red and green curves that represent the background and the subprocess $\mathcal{E}_{miss} \equiv \bar{\nu}_e \nu_\mu$ can not be seen due to the considered range. The curves $N_i N_3$ are the only non-negligible contributions that can be presented for the benchmark in (3).

As a Benchmark, we consider the following set of the model parameter values:

$$\begin{aligned}
 f_{e\mu} &= -(4.97 + i1.41) \times 10^{-2}, \quad f_{e\tau} = 0.106 + i0.0859, \quad f_{\mu\tau} = (3.04 - i4.72) \times 10^{-6}, \\
 g_{i\alpha} &= 10^{-2} \times \begin{pmatrix} 0.2249 + i0.3252 & 0.0053 + i0.7789 & 0.4709 + i1.47 \\ 1.099 + i1.511 & -1.365 - i1.003 & 0.6532 - i0.1845 \\ 122.1 + i178.4 & -0.6398 - i0.6656 & -10.56 + i68.56 \end{pmatrix}, \\
 m_{N_i} &= \{162.2 \text{ GeV}, 182.1 \text{ GeV}, 209.8 \text{ GeV}\}, \quad m_{S_i} = \{914.2 \text{ GeV}, 239.7 \text{ GeV}\},
 \end{aligned} \tag{3}$$

which has all the features listed in the previous section. For this benchmark, the only kinematically allowed decay modes of $N_{2,3}$ are three-body decays and therefore their total decay widths are small. This means, they might decay outside the detector, and therefore their signatures is similar to the of N_1 . Detailed studies about the production mechanisms and the decay modes in e^+e^- collisions, of new heavy fermions and neutrinos has been performed in [17]. Furthermore, the analysis of various signals and backgrounds of new heavy fermions predicted by the SM extensions can be found in [18].

In our model, the missing energy in the process $e^-e^+ \rightarrow e^-\mu^+ + E_{miss}$ corresponds to any state in the set $\mathcal{E}_{miss} \subset \{\nu_\mu \bar{\nu}_e, \nu_e \bar{\nu}_\tau, \nu_\tau \bar{\nu}_e, \nu_\mu \bar{\nu}_\mu, \nu_\tau \bar{\nu}_\mu, \nu_\tau \bar{\nu}_\tau, N_i N_k; i, k = 1, 2, 3\}$. The total expected cross section of the processes $e^-e^+ \rightarrow e^-\mu^+ + E_{miss}$ is represented by σ^{EX} , while $\sigma(\mathcal{E}_{miss})$ denotes the cross section of different subprocesses.

The background comprises two leptons (electron and anti-muon) plus missing energy $E_{miss}^{(SM)} \equiv \bar{\nu}_e \nu_\mu$. In our model, the subprocess $\mathcal{E}_{miss} \equiv \nu_\mu \bar{\nu}_e$ has 22 diagrams mediated by S_1 in addition to the 18 diagrams that exist in the SM. Then, the number of signal events is the difference between the contributions from the 12 subprocesses mentioned above and the SM background. Hence, our goal will be to study the feasibility of detecting any possible excess of events in our model compared to the SM predictions at the International Linear Collider (ILC) [8–10, 19] for different beam energies. Our analysis also applies to the other future leptonic linear colliders, such as Compact Linear Collider (CLIC) [12]; and the Triple-Large Electron-Positron Collider (TLEP) [11].

For small beam energies (such as 250 or 350 GeV), the RH neutrinos can not be produced due to the kinematical constraints; and when there are any observed events from the defined signal, it is due to the light LH neutrinos. However, at higher energies up to around 1 TeV, one expects the heavy RH neutrinos (N_i) to be pair produced and therefore contribute significantly to the total cross section of the process $e^-e^+ \rightarrow e^-\mu^+ + E_{miss}$. In this case, the energy of the muon and/or electron is expected to be smaller than the case where the missing energy is LH neutrinos.

Fig. 2 shows the cross section for each subprocess versus the CM energies $E_{CM} = 250 \sim 1000$ GeV using unpolarized beams for the considered model parameters given in (3). Among the different contributions to the total missing energy, the cross section for the final states $\mathcal{E}_{miss} \subset \{\nu_e \bar{\nu}_\tau, \nu_\tau \bar{\nu}_e, \nu_\mu \bar{\nu}_\mu, \nu_\tau \bar{\nu}_\mu, \nu_\tau \bar{\nu}_\tau, N_1 N_1, N_1 N_2, N_2 N_2\}$ are found to be negligible. In Fig. 2, we show the plot of $\sigma(\mathcal{E}_{miss} \equiv N_i N_3)$, with $i = 1, 2, 3$, versus the CM energy, which shows that $\sigma(\mathcal{E}_{miss} \equiv N_3 N_3)$ is much larger than both $\sigma(\mathcal{E}_{miss} \equiv N_1 N_3)$ and $\sigma(\mathcal{E}_{miss} \equiv N_2 N_3)$. Then at low CM energies, the signal in this model, comes only from the subprocess $e^+ + e^- \rightarrow e^-\mu^+ \nu_\mu \bar{\nu}_e$, i.e., the diagrams that are mediated by the charged scalar S_1 . At higher values of E_{CM} , there could be additional contributions from the subprocesses $e^+ + e^- \rightarrow e^-\mu^+ N_i N_3$, which are mediated by the charged scalar S_2 .

The contributions of $N_{1,2}N_{1,2}$ are negligible due to the constraints from neutrino oscillation data, LFV processes, and the DM relic density. This requires the couplings $g_{1\alpha}$ and $g_{2\alpha}$ to be very small compared to $g_{3\alpha} \sim \mathcal{O}(1)$ [6]. Moreover, the contributions $\{\nu_e\bar{\nu}_\tau, \nu_\tau\bar{\nu}_e, \nu_\mu\bar{\nu}_\mu, \nu_\tau\bar{\nu}_\mu, \nu_\tau\bar{\nu}_\tau\}$ are also negligible due to the smallness of the couplings $f_{\alpha\beta}$ in addition to the large value of m_{S_1} . Consequently, the highly suppressed interactions mediated by S_1 , makes to the cross section $\sigma(\mathcal{E}_{miss} \equiv \nu_\mu\bar{\nu}_e)$ very close to the background as illustrated in Fig. 2.

In order to maximize the signal detection, one has to choose a set of cuts where the signal significance should be larger than 3σ . The general significance definition is defined by

$$S = N_S / \sqrt{N_S + N_B}, \quad (4)$$

where N_S and N_B are the signal and background events number, respectively. Here N_S is given by

$$N_S = N_{EX} - N_B = L \times (\sigma^{EX} - \sigma^{BG}), \quad (5)$$

with N_{EX} is the expected events number, L is the integrated luminosity and σ^{EX} (σ^{BG}) is the expected (background) cross section within the considered cuts.

One of the powerful characteristics of future e^+e^- linear colliders, such as the ILC, is the possibility of having the electron and/or positron beams being polarized [19, 20]. This feature can be used to reduce the background contribution which can result in a significant improvement of the signal to background ratio. At the ILC, both electron and positron polarizations are chosen to lie in the range [20]

$$|P(e^-)| \leq 0.8; \quad |P(e^+)| \leq 0.3, \quad (6)$$

with $P(f) = (N_{f_R} - N_{f_L}) / (N_{f_R} + N_{f_L})$; and N_{f_R} (N_{f_L}) is the number of right (left) handed fermions. For CLIC, the positron polarization could reach up to $|P(e^+)| = 0.6$, therefore one expects the background to be more suppressed [21]. Hence, by considering the electron (positron) polarization $P(e^-) < 0$ ($P(e^+) > 0$), the excess in the number of LH (RH) neutrino events gets enhanced.

We will carry out our simulation based on the benchmark (3), and use the ILC run at different CM energy: $E_{CM} = 250, 350, 500$ GeV and 1 TeV, with unpolarized beams at first; then we consider the polarized beams with $P(e^-, e^+) = [-0.8, +0.3]$ and/or $P(e^-, e^+) = [+0.8, -0.3]$. The details of our analysis is described throughout the next section.

IV. ANALYSIS AND DISCUSSION

In this work, we used LanHEP [22] and CalcHep [23] for the simulation of our model; and generated the differential cross section with respect to all the relevant kinematic variables. We found that the expected cross section is barely larger than the background $\sigma^{EX} \gtrsim \sigma^{BG}$; and the distributions have the same shape. We found out that the useful kinematic variables, where the events number excess can be remarkable are: the charged leptons energy (E_ℓ), angular distributions ($\cos\theta_\ell$), the invariant mass ($M_{e,\mu}$); and the missing invariant mass (M_{miss}). The latter variable can be reconstructed fairly at any lepton collider since the full information about the initial state momenta are provided. A summary of the considered cut sets is shown in Table-I.

E_{CM}	Selection cuts
250	$70 < E_\ell < 110$, $70 < M_{e,\mu} < 220$, $M_{miss} < 120$, $0.4621 < \cos\theta_e < 0.9640$, $-0.9640 < \cos\theta_\mu < -0.4621$,
350	$90 < E_\ell < 165$, $100 < M_{e,\mu} < 280$, $M_{miss} < 200$, $0.4621 < \cos\theta_e < 0.9951$, $-0.9866 < \cos\theta_\mu < 0$,
500	$120 < E_\ell < 240$, $300 < M_{e,\mu} < 480$, $M_{miss} < 300$, $0.4621 < \cos\theta_e < 0.9951$, $-0.9951 < \cos\theta_\mu < 0$,
1000	$E_\ell < 70$, $M_{e,\mu} < 140$, $M_{miss} > 750$, $0.0997 < \cos\theta_e < 0.6640$, $-0.6640 < \cos\theta_\mu < -0.0997$.

TABLE I: Relevant cuts for the process $e^+e^- \rightarrow E_{miss} + e^-\mu^+$ at different CM energies. Here E_ℓ and θ_ℓ are the charged lepton energy in emission angles, $M_{e,\mu}$ is the electron-muon invariant mass and M_{miss} is the missing invariant mass. All masses and energies are given in GeV.

From the angular cuts at different CM energies in Table-I, the charged leptons from the process $e^+ + e^- \rightarrow e^-\mu^+ + E_{miss}$ could be emitted in wide angle ranges, while in a similar model studied in [13], the outgoing leptons

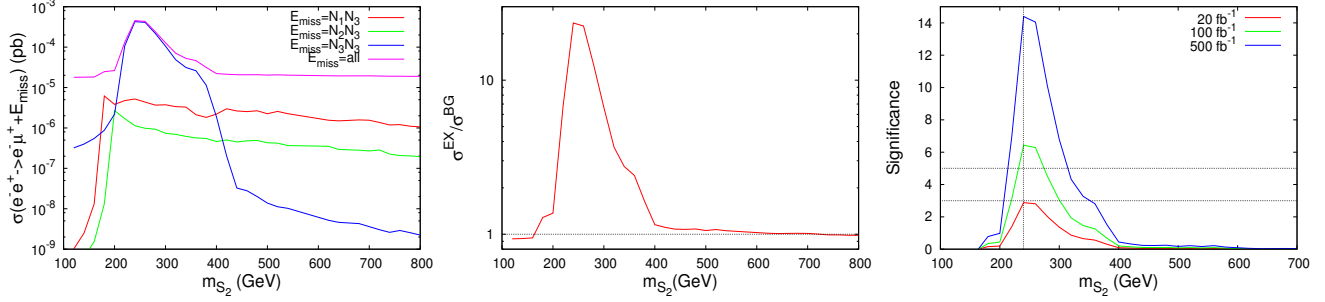


FIG. 3: These plot are obtained for $E_{CM}=1$ TeV within the cuts given in Table-I. Left panel: the cross section of different subprocess as a function of the charged scalar masses m_{S_2} . Middle panel: the expected cross section σ^{EX} scaled by the background. Right panel: the significance (\mathcal{S}) versus m_{S_2} for different integrated luminosity values, where the two dashed horizontal lines represent the values $\mathcal{S} = 3$ and $\mathcal{S} = 5$, respectively; and the vertical one represents the physical value of the charged scalar mass m_{S_2} (given in (3)).

(e^- and μ^+) are emitted almost collinearly. This is due to the fact that in our model the process proceeds via both t - and s -channel whereas in [13] it is via only the t -channel.

By imposing the cuts in Table-I at each CM energy, we obtain both the expected signal and the background cross sections. This gives us an idea about the required luminosity from the significance values as presented in Table-II.

E_{CM}	σ^{BG}	σ^{EX}	$(\sigma^{EX} - \sigma^{BG}) / \sigma^{BG}$	\mathcal{S}_{100}	\mathcal{S}_{500}
250	6.5919×10^{-2}	6.7402×10^{-2}	2.2497×10^{-2}	1.8064	4.0391
350	5.8882×10^{-2}	6.0158×10^{-2}	2.2723×10^{-2}	1.6451	3.6787
500	5.6560×10^{-2}	5.7630×10^{-2}	1.8918×10^{-2}	1.4095	3.1517
1000	1.9217×10^{-5}	4.6976×10^{-4}	23.445	6.5735	14.699

TABLE II: The cross sections of the total expected signals and the background estimated for the considered energies within the cuts given in Table-I; and the significance \mathcal{S}_{100} and \mathcal{S}_{500} that correspond to the two integrated luminosity values $L=100, 500 \text{ fb}^{-1}$, respectively. All energies are given in GeV and cross sections in pb.

One has to mention that for $E_{CM} = 250, 350$ and 500 GeV, the corresponding required luminosity to detect the signal should be higher than the values reported in [10], in contrast to the case where $E_{CM} = 1$ TeV. As can be seen from the cuts on the charged leptons energy and the missing invariant mass in Table-I in addition to the cross sections in Table-II, clearly the events number excess at $E_{CM} = 1$ TeV has different source compared to the other CM energies. Here, the missing energy is mainly RH Majorana neutrinos; due to the following reasons: (1) The missing invariant mass is large because N_3 is very massive, (2) the existence of heavy RH neutrinos in the final state leads to small phase space for the daughter particles including the charged leptons; and (3) the expected cross section is dominated by the subprocess $\mathcal{E}_{miss} \equiv N_3 N_3$, whereas the $\mathcal{E}_{miss} \equiv \nu_\mu \bar{\nu}_e$ contribution is comparable to the background.

Note that there are 34 Feynman diagrams that contribute to the amplitude of the subprocess $e^- e^+ \rightarrow e^- \mu^+ + N_3 N_3$, all of them mediated by the charged scalar S_2 . Then, in Fig. 3, we illustrate the cross sections of the different $\mathcal{E}_{miss} \equiv N_i N_3$ subprocesses, and the corresponding significance versus the charged scalar mass m_{S_2} .

Moreover in Fig. 3, the cross section $\sigma(\mathcal{E}_{miss} \equiv N_3 N_3)$ gets enhanced for charged scalar mass near the resonance value $m_{S_2} \sim 240$ GeV, whereas it is negligible elsewhere. It is interesting to notice that m_{S_2} value in our benchmark (3) corresponds exactly the resonance. Here again by looking at the charged scalar masses $m_{S_2} < 164$ GeV and $m_{S_2} > 724$ GeV, the cross section σ^{EX} is expected to be smaller than the background; and therefore there is no significant events number excess that can be observed in this case.

Now, we extend our study by considering polarized beams in order to increase the signal to the background. Hence, we consider $P(e^-, e^+) = [-0.8, +0.3]$ for $E_{CM} = 250, 350$ and 500 GeV and $P(e^-, e^+) = [+0.8, -0.3]$ for $E_{CM} = 1$ TeV. Keeping the same defined cuts listed in Table-I, the estimated cross section and significance values presented in Table-II get modified, as summarized in Table-III.

From Table-III, after using the polarization, the expected cross section gets enhanced by about 150% for $E_{CM} = 250, 350, 500$ GeV and by about 50% for $E_{CM} = 1$ TeV. This makes the signal easy to detect for all the considered CM energies. As a summary, we give in Table-IV the expected events number excess for each CM energy with and without polarized beams. In Fig. 4, we show the dependance of the significance on the

E_{CM}	$P(e^-, e^+)$	σ^{BG}	σ^{EX}	$(\sigma^{EX} - \sigma^{BG}) / \sigma^{BG}$	\mathcal{S}_{100}	\mathcal{S}_{500}
250	-0.8, +0.3	0.15399	0.15910	3.3184×10^{-2}	4.0512	9.0588
350	-0.8, +0.3	0.13640	0.13997	2.6173×10^{-2}	3.0175	6.7474
500	-0.8, +0.3	0.13100	0.13450	2.6718×10^{-2}	3.0179	6.7483
1000	+0.8, -0.3	2.0708×10^{-6}	7.2710×10^{-4}	350.12	8.5027	19.013

TABLE III: The cross sections for the total expected signals and the background estimated for the considered energies within the cuts given in Table-I; and the significance \mathcal{S}_{100} and \mathcal{S}_{500} that correspond to the two integrated luminosity values $L=100, 500 \text{ fb}^{-1}$, respectively. All energies are given in GeV and cross sections in pb.

$E_{CM} \text{ (GeV)}$	$L \text{ (fb}^{-1}\text{)}$	$P(e^-, e^+)$	N_B	N_{EX}	N_S
250	250	0, 0	16480	16851	371
		-0.8, +0.3	38498	39775	1277
350	350	0, 0	20609	21055	446
		-0.8, +0.3	47740	48990	1250
500	500	0, 0	28280	28815	535
		-0.8, +0.3	65500	67250	1750
1000	1000	0, 0	19.217	469.76	450.54
		+0.8, -0.3	2.07	727.10	725.03

TABLE IV: The expected (N_{EX}) and background (N_B) number of events for different CM energy values with/without polarized beams within the cuts given in Table-I.

accumulated luminosity with and without polarized beams for the considered CM energies, within the cuts given in Table-I. Thus, we see that by having a polarized beam, the signal can be observed even with relatively low integrated luminosity. For example, at $E_{CM} = 250 \text{ GeV}$, the 5σ required luminosity is 150 fb^{-1} for polarized beam as compared to 700 fb^{-1} without polarization.

V. CONCLUSIONS

In this work, we have studied the detectability of a radiative model for neutrino masses at the future e^-e^+ linear colliders. At different CM energies $E_{CM}=250, 350, 500 \text{ GeV}$ and 1 TeV , we studied the process $e^-e^+ \rightarrow e^-\mu^+ + E_{miss}$. We found that for the CM energies 250, 350 and 500 GeV, the missing energy is mainly light LH neutrinos, while at $E_{CM} = 1 \text{ TeV}$, the RH neutrinos contribution is dominant.

We have shown for the CM energy $E_{CM} = 1 \text{ TeV}$, the signal is sensitive to the mass of the charged scalar m_{S_2} ; and it is only significant near a resonant value $m_{S_2} \sim 240 \text{ GeV}$, which corresponds to the value chosen in our benchmark.

We found that the signal can not be seen at $E_{CM}=250, 350, 500 \text{ GeV}$ in contrast the case of $E_{CM} = 1 \text{ TeV}$. After using polarized beams, the signal gets enhanced and can be observed for all CM energies. Furthermore, when considering polarization, the signal can be detected with smaller integrated luminosity as compared to unpolarized beam case.

Acknowledgments

We thank the ICTP and CERN for their hospitality where a large part of this work has been carried out. We thank S. Kanemura for useful discussions during early stages of this work, and K. Yagyu for reading the manuscript. Special thanks to A. Djouadi for the careful reading and the very useful discussions. The work of A. A. is supported by the Algerian Ministry of Higher Education and Scientific Research under the PNR '*Particle Physics / Cosmology: the interface*'; and the CNEPRU Project No. D01720130042.

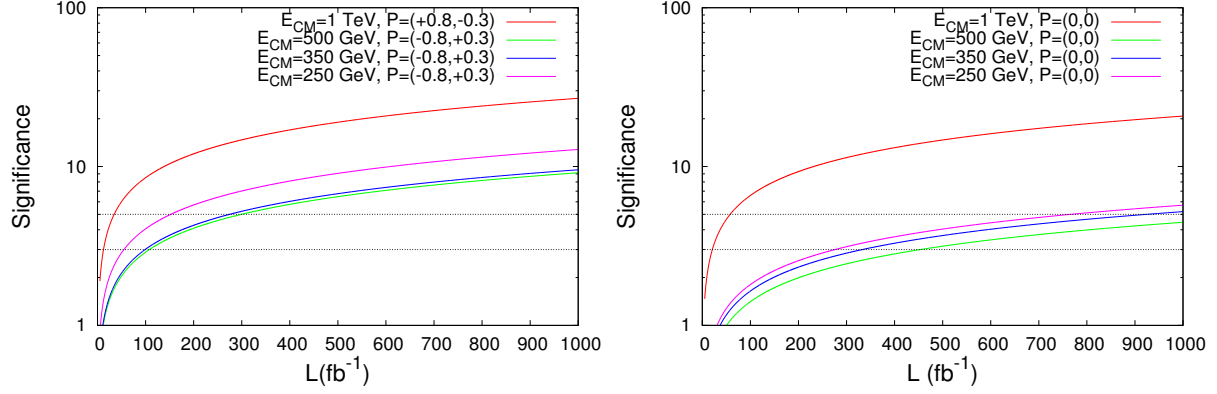


FIG. 4: The significance versus luminosity at different CM energies within the cuts defined in Table-I; with (left) and without (right) polarized beams. The two horizontal dashed lines represent $\mathcal{S} = 3$ and $\mathcal{S} = 5$, respectively.

- [2] P.A.R. Ade et al. [Planck Collaboration], arXiv:1303.5062 [astro-ph.CO].
- [3] A. D. Sakharov, Pisma Zh. Eksp. Teor. Fiz. 5, 32 (1967).
- [4] L.M. Krauss, S. Nasri and M. Trodden, Phys. Rev. D 67, 085002 (2003).
- [5] K. Cheung and O. Seto, Phys. Rev. D 69, 113009 (2004).
- [6] A. Ahriche and S. Nasri, JCAP 1307, 035 (2013).
- [7] M. Aoki, S. Kanemura and O. Seto, Phys. Rev. Lett. 102, 051805 (2009); Phys. Rev. D 80, 033007 (2009); M. Aoki, S. Kanemura and K. Yagyu, Phys. Rev. D 83, 075016 (2011).
- [8] J. Brau, Y. Okada, N. Walker et al. (ILC Collaboration), arXiv:0712.1950 [physics.acc-ph].
- [9] A. Djouadi, J. Lykken, K. Monig, Y. Okada, M. Oreglia, S. Yamashita et al. (ILC Collaboration), arXiv:0709.1893 [hep-ph].
- [10] N. Phinney, N. Toge, N. Walker et al. (ILC Collaboration), arXiv:0712.2361 [physics.acc-ph].
- [11] G. Gomez-Ceballos et al., JHEP 01, 164 (2014).
- [12] The CLIC Study Team, Report No. CERN 2000-008, 2000; E. Accomando et al. (CLIC Physics Working Group Collaboration), arXiv:hep-ph/0412251.
- [13] S. Kanemura, T. Nabeshima and H. Sugiyama, Phys. Rev. D 87, 015009 (2013).
- [14] S.-Y. Ho and J. Tandean, arXiv:1312.0931 [hep-ph].
- [15] G. Aad et al. (ATLAS Collaboration), Phys. Lett. B 716, 1-29 (2012).
- [16] S. Chatrchyan et al. (CMS Collaboration), Phys. Lett. B 716, 30-61 (2012).
- [17] A. Djouadi, Z. Phys. C 63, 317 (1994).
- [18] A. Djouadi, Z. Phys. C 63, 327 (1994).
- [19] T. Behnke, C. Damerell, J. Jaros, A. Miyamoto et al. (ILC Collaboration), arXiv:0712.2356 [physics.ins-det].
- [20] C. Adolphsen, M. Barone, B. Barish, K. Buesser, Ph. Burrows, J. Carwardine, J. Clark, H.M. Durand, G. Dugan, E. Elsen et al. arXiv:1306.6328 [physics.acc-ph].
- [21] R.W. Assmann and F. Zimmermann, talk given at Snowmass 2001; W. Liu, W. Gai, L. Rinolfi and J. Sheppard, Conf. Proc. C 100523, THPEC035 (2010).
- [22] A. Semenov, Comput. Phys. Commun. 180, 431 (2009).
- [23] A. Belyaev, N. Christensen and A. Pukhov, Comput. Phys. Commun. 184, 1729 (2013).